

## Original Research

# A Rat Model of Diabetic Wound Infection for the Evaluation of Topical Antimicrobial Therapies

João J Mendes,<sup>1,2,\*</sup> Clara I Leandro,<sup>2</sup> Dolores P Bonaparte,<sup>3</sup> and Andreia L Pinto<sup>4</sup>

Diabetes mellitus is an epidemic multisystemic chronic disease that frequently is complicated by complex wound infections. Innovative topical antimicrobial therapy agents are potentially useful for multimodal treatment of these infections. However, an appropriately standardized *in vivo* model is currently not available to facilitate the screening of these emerging products and their effect on wound healing. To develop such a model, we analyzed, tested, and modified published models of wound healing. We optimized various aspects of the model, including animal species, diabetes induction method, hair removal technique, splint and dressing methods, the control of unintentional bacterial infection, sampling methods for the evaluation of bacterial burden, and aspects of the microscopic and macroscopic assessment of wound healing, all while taking into consideration animal welfare and the '3Rs' principle. We thus developed a new wound infection model in rats that is optimized for testing topical antimicrobial therapy agents. This model accurately reproduces the pathophysiology of infected diabetic wound healing and includes the current standard treatment (that is, debridement). The numerous benefits of this model include the ready availability of necessary materials, simple techniques, high reproducibility, and practicality for experiments with large sample sizes. Furthermore, given its similarities to infected-wound healing and treatment in humans, our new model can serve as a valid alternative for applied research.

**Abbreviations:** DG, dermal gap; DM, diabetes mellitus; EG, epithelial gap; GT, granulation tissue; TAT, topical antimicrobial therapy.

The world is facing a growing diabetes mellitus (DM) epidemic, and diabetic foot ulcers, with an estimated lifetime risk of 25%,<sup>40</sup> constitute one of the most common complications of this disease. About 58% of ulcers become clinically infected,<sup>32</sup> often leading to amputation. Diabetic wounds<sup>6,13</sup> do not follow the precisely orchestrated course of events observed in normal healing, and bacterial colonization or infection further disrupts this process.<sup>14</sup> In current clinical practice, once an adequate blood supply is assured, the treatment of diabetic foot infections includes debridement, systemic antibiotics, and dressings.<sup>24</sup> Mechanical debridement is pivotal to this strategy, because it not only significantly reduces the bioburden but also opens a time-dependent therapeutic window for topical antimicrobial therapy (TAT).<sup>50</sup> TAT agents consist of an active antimicrobial molecule associated with a vehicle or base, thereby delivering a high and sustained antibiotic concentration directly to the site of infection while avoiding systemic toxicity.<sup>25</sup>

Several new TAT agents are under investigation, and a phased strategy of efficacy and toxicity testing is required before they can be made widely available for human use. None of the presently available *in vitro* or *in vivo* models of wound healing is optimal. As experimental models, *in vitro* tests fail to reproduce the physiologic and pathogenic complexity of an organism, making *in vivo* models a crucial tool for ensuring clinical relevance.<sup>36</sup>

Researchers have studied *in vivo* wound healing in a variety of species, including pigs,<sup>48</sup> rabbits,<sup>1</sup> rats,<sup>12,35,46</sup> and mice,<sup>6,47</sup> by using different incisional, excisional, and granulation wound models in animals rendered diabetic through genetic modification or chemical induction.

For most researchers, rodents are the model of choice because they are inexpensive, easy to handle, require little space, and have accelerated healing compared with humans, thereby yielding for faster results.<sup>36</sup> The excisional wound model accommodates the broadest assessment of the mechanisms involved in wound healing, including epithelialization, granulation, and angiogenesis.<sup>51</sup> In addition, this model supports the evaluation of new topical pharmacologic interventions because medications can be applied directly to the wound bed.<sup>46,47</sup> All models of excisional wound healing are based on the same principles (Figure 1).<sup>36</sup> However, these models have been criticized because the main mechanism of wound healing in rodents is contraction<sup>16</sup> due to the presence of the panniculus carnosus muscle in the subcutaneous tissue; in contrast, humans heal more through reepithelialization.<sup>14</sup> One rodent excisional wound healing model minimizes wound contraction by the use of silicone splints that are fixed to the skin by using immediate-bonding adhesive and nylon sutures.<sup>16</sup> Although potentially useful for evaluating diabetic wound bacterial infections, this model has not been tested or validated in this context. Other published animal models of infected cutaneous wounds<sup>39,54</sup> fail to afford the optimal characteristics of the model cited previously.<sup>16</sup> Still, this model<sup>16</sup> is not without disadvantages, namely the difficulty of applying and maintaining the dressing (and splint) while maintaining stringent infection control.

Received: 17 Aug 2011. Revision requested: 14 Sep 2011. Accepted: 13 Oct 2011.

<sup>1</sup>Internal Medicine Department, Hospital de Santa Marta/Centro Hospitalar de Lisboa Central EPE, <sup>2</sup>TechnoPhage, <sup>3</sup>Animal Facility and <sup>4</sup>Histology Service, Instituto de Medicina Molecular, Lisbon, Portugal.

\*Corresponding author. Email: joaojoamendes@hotmail.com

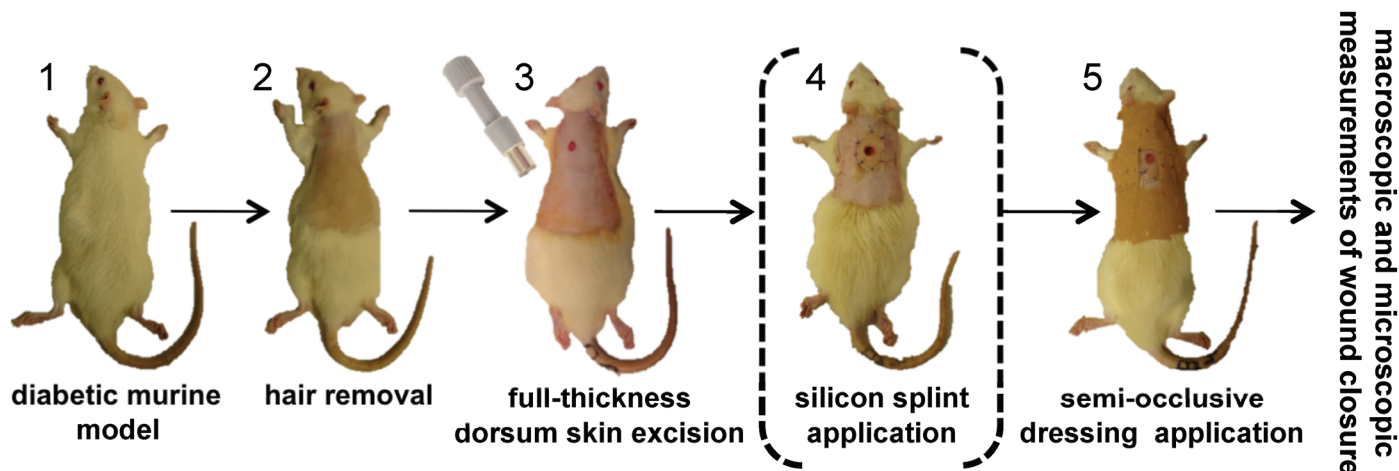


**Figure 1.** Schematic representation of diabetic rodent models of excisional wound healing. (1) Genetically modified or chemically induced diabetic animals are used. (2) Hair is removed (various techniques are available). (3) A full-thickness wound extending through the panniculus carnosus is created in the interscapular region of the upper back, typically by using a punch biopsy instrument. (4) Some models use a silicone splint fixed to the skin, for minimizing wound contraction while allowing the normal granulation and reepithelialization. (5) The wound is covered with a semioclusive dressing. Various macroscopic and microscopic methods are available for the evaluation of wound closure.

Because, to our knowledge, better *in vivo* models are not available for the evaluation of TAT in diabetic wound infections, we refined and adapted the previous murine model<sup>16</sup> to develop a useful and cost-effective model for this purpose.

## Materials and Methods

This study was approved locally by the Animal Ethics Committee of the Instituto de Medicina Molecular and nationally by the Portuguese General Directorate of Veterinary Services (Direcção Geral de Veterinária), in accordance with Portuguese law. All animals were maintained in accordance with European Directive 86/609/EC,<sup>10</sup> Portuguese law (Portaria 1005/92),<sup>31</sup> and the *Guide for the Care and Use of Laboratory Animals*.<sup>21</sup> This study included the refinement and optimization of several sequential procedures. The animals used and the DM induction protocol were the same for all study groups. The final optimized wound-infection model study was preceded by 3 sequential optimization studies: hair removal (optimization study 1); prevention of unintentional critical colonization (optimization study 2); and assessment of wound bioburden (optimization study 3). To reduce the number of study groups, and therefore the total number of animals, each subsequent optimization study incorporated the findings of previous studies.

**Animals.** Specific pathogen-free male Wistar rats (CrI:WI[Han]; weight, 250 to 350 g; age, 8 to 10 wk) were obtained from Charles River Laboratories (L'Arbresle Cedex, France) and kept in an approved animal care center. The rats were maintained in microisolation caging in a room with controlled humidity (50% to 70%) and temperature (20 to 22 °C), a 14:10-h light:dark cycle, and free access to pelleted rodent chow (RM3, Special Diet Systems, Essex, UK) and filter-sterilized water. Initially housed in groups of 2, rats were housed individually after hair removal to preserve skin and dressing integrity.

**Induction of DM.** DM was induced chemically as described previously.<sup>52</sup> Briefly, after a 12-h fast, rats received a single intraperitoneal injection of streptozotocin (65 mg/kg; Merck Chemical, Darmstadt, Germany) freshly prepared in 0.1 M sodium citrate

buffer (pH 4.5). At 8 d after streptozotocin injection, blood glucose measurement was performed on tail-vein blood by using a glucometer (Accu-Chek Aviva Nano, Roche Diagnostics, Penzberg, Germany). Rats whose fasting blood glucose levels exceeded 250 mg/dL (13.9 mmol/dL) were considered diabetic. Water intake and weight were monitored throughout the study, and to confirm the diabetic state, fasting blood glucose measurement was repeated on the day of euthanasia.

**Optimization study 1: hair removal.** On the day of DM confirmation, 9 diabetic rats were anesthetized by intraperitoneal injection of xylazine hydrochloride (10 mg/kg) and ketamine hydrochloride (25 mg/kg), and their dorsal surface hair was trimmed with an electric clipper. Rats then were divided into 3 groups depending on the method used to remove any remaining hair: straight razor; 2) depilatory cream (Opilca, GlaxoSmithKline Consumer Healthcare, Copenhagen, Denmark); and 3) cold wax (Veet cold wax strips, Reckitt Benckiser, West Ryde, Australia). The dorsum of all rats was rinsed with a 10% povidone-iodine solution and, after drying and cleansing, a liquid film-forming acrylate (Cavilon Skin Cleanser, 3M Health Care, Saint Paul, MN) was applied evenly to cover the hair removal area. A photograph of the dorsum of the rat was taken from a 1.5 cm standard height (ES65 digital camera, Samsung, Beijing, China), and the rats were placed on a 37 °C heating pad to minimize hypothermia. All rats received sterile sodium chloride to prevent dehydration. After fully recovering from anesthesia, rats were placed in individual cages. Photographs of nonanesthetized rats were taken on days 4 and 14 after hair removal and used by 3 independent observers for evaluation of the hair-density index (scale: 1 [no hair] to 5 [normal amount of hair]) and skin-damage index (scale: 1, intact skin; 2, erythematous skin; 3, epidermal injury; 4, dermal injury; and 5, subcutaneous layer injury). Hair density and skin damage scores are expressed as the median (first and third quartiles).

**Optimization study 2: prevention of unintentional critical colonization.** Based on the findings of the previous optimization study, 18 Wistar rats with chemically induced DM were epilated by using cold wax and anesthetized by intraperitoneal injection of xylazine-ketamine 4 d thereafter.

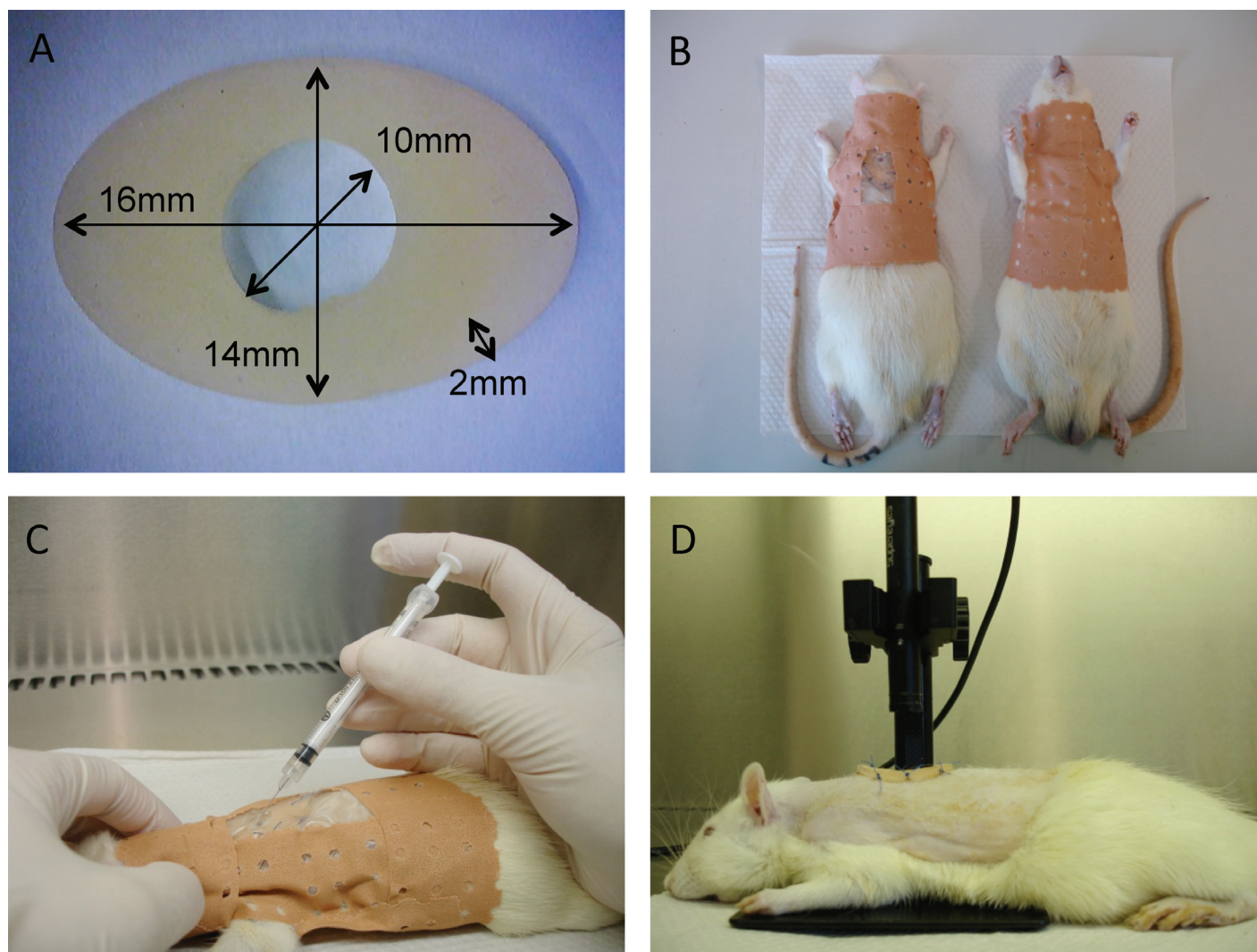


**Figure 2.** Illustration of specific techniques. (A) The oval-shaped silicone splint and its dimensions. (B) Application of a jacket made from adhesive tape to prevent dressing loss. (C) Bacterial inoculation of the wound bed by inserting a 27-gauge, 19-mm needle attached to a 1-mL disposable syringe through the silicon splint at a 45° angle. (D) Wounds photographed from a standard 1.5 cm height by using a mounted digital microscope.

**Decontamination protocols.** All surgical procedures were performed in a sanitized surgery room by using autoclave-sterilized instruments. Because the procedures were repeated in multiple rats, 2 sets of instruments were used. Between uses, instruments were cleaned thoroughly to remove all organic debris, disinfected with a multipurpose disinfectant (Virkon, Antec International Limited, Suffolk, UK), and resterilized by using a glass bead sterilizer (FST 250, Fine Science Tools, North Vancouver, **Canada**) according to the manufacturer's guidelines. The surgeon wore clean scrubs, mask, and hair cap and used fresh sterile gloves for each rat.

**Wounding, splinting, and dressing.** The anesthetized rats were separated into 3 groups depending on the method of decontamination of the dorsal skin: thorough washing with sterile saline only; thorough washing with sterile saline followed by disinfection with 10% povidone-iodine; and sterile saline plus povidone-iodine (10 min contact time) followed by 70% isopropyl alcohol. A punch biopsy instrument (diameter, 6 mm; Accu-Punch, Acuderm, Fort Lauderdale, USA) then was used to create a full-thick-

ness round wound extending through the panniculus carnosus in the interscapular region of the upper back of each rat, and the skin flap was excised by using iris scissors. An oval-shaped silicone splint (Figure 2 A) was adapted from a self-adhesive corn cushion (Comforsil, Toledo, Spain). Immediate-bonding cyanoacrylate glue in a disposable single-dose package (Loctite, Henkel Corporation, Westlake, OH) was used to fix the splint to the skin, followed by interrupted 3-0 nylon sutures to ensure its position. Liquid film-forming acrylate was applied to the epilated area, and the wound and surrounding area were covered with a previously tailored, semioclusive, nonwoven polyester dressing (Fixomull Stretch, BSN Medical, Hamburg, Germany). The splint and dressing were maintained in place throughout the entire course of the experiment by the use of a jacket (Figure 2 B) made from adhesive tape (Leukoplast surgical tape, BSN Medical).

**Debridement of the ulcer and assessment of contamination.** Four days after wounding, the semioclusive dressing was removed, and a scab, defined as a crust of dried blood, serum, and exudate,<sup>54</sup> was noted over each wound. By using strict aseptic

technique, the ulcer was debrided by simple mechanical removal of the scab. The ulcer then was photographed as previously described, and a liquid Amies elution swab (eSwab Collection and Preservation System, Copan, Corona, CA) was used to collect and transport swab cultures. Bacteria collection was performed by using the one-point method.<sup>45</sup> Briefly, by using the sterile swab, the center surface of each wound was scrubbed carefully by rotating the swab 3 times clockwise with enough manual pressure to produce a small amount of exudate. The inoculated swab was inserted into a tube containing 1 mL liquid Amies transport medium and transported to the laboratory for immediate processing. The swab collection tube was vortexed (with the swab inside) for 5 s, and a 100- $\mu$ L aliquot of the suspension was used for serial dilutions. Quantification of the viable bacteria present in the swab was performed by using the 10-fold serial dilution method,<sup>28</sup> and 100  $\mu$ L of each dilution was plated onto tryptone soy agar (Biokar Diagnostics, Pantin Cedex, France). The plates were incubated under aerobic conditions at 37 °C for 24 h, after which colony-forming units were counted. The wound and surrounding area again were covered with a previously tailored, semiocclusive, nonwoven polyester dressing. Because all of these procedures are considered to be painless and noninvasive, they were performed on unanesthetized rats. A surgical drape was placed over the head of the rat to reduce stress and ensure immobilization. The entire procedure (including debridement) was repeated on days 5, 8, and 11. Rats were evaluated twice daily for the integrity of the adhesive jacket, which was reinforced whenever deemed necessary. On day 11, the rats were euthanized by intraperitoneal injection of pentobarbital (200 mg). Quantitative microbiologic results were expressed as the number of colony-forming units per swab and, on the basis of previous studies<sup>33</sup> and the results of optimization study 3, rats with more than 10<sup>3</sup> cfu/swab on any given day were considered to be critically colonized. Results are presented as unit values and percentages.

**Optimization study 3: assessment of wound bioburden.** For this experiment, 14 Wistar rats with chemically induced DM were epilated by using cold wax, and an incision was made in each rat, splinted, and dressed as previously optimized and described. These ulcers were inoculated with bacterial suspensions of either *Staphylococcus aureus* or *Pseudomonas aeruginosa*. Clinical strains of *S. aureus* and *P. aeruginosa* that previously had been isolated from patients with chronic skin ulcers and cryopreserved at -70 °C were grown on tryptone soy agar. After 24 h, bacterial cultures were harvested, and a bacterial suspension was prepared and compared with a McFarland standard (bioMérieux, Crajonne, France). The inoculation dose was approximately 2.0  $\times$  10<sup>7</sup> cfu/mL. The rats were divided into 2 groups of 7 animals each (*S. aureus* and *P. aeruginosa*). After application of the dressing and with the rat still anesthetized, the wound bed was inoculated with 100  $\mu$ L of cultured bacteria (approximately 2.0  $\times$  10<sup>6</sup> cfu) resuspended in sterile saline by inserting a 27-gauge, 19-mm needle attached to a 1-mL disposable syringe through the silicon splint at a 45° angle (Figure 2 C).

At 4 d after wounding, rats were euthanized by intraperitoneal injection of pentobarbital (200 mg), the semiocclusive dressing was removed, the ulcer was debrided, and a swab was obtained as described previously. Then, by using sterile surgical scissors, each wound was harvested in its entirety and placed in a sterile tube. Swabs and tissue samples were transported to the laboratory for immediate processing. The swabs were processed as pre-

viously described, and tissue samples were homogenized in 5 mL sterile saline in a pearl jar, vortexed for 20 s, and sonicated for 90 s at 35 MHz (Transsonic T570, Elma, Singen, Germany) to disaggregate bacteria (this procedure had been optimized previously to minimize cell disruption). A 100- $\mu$ L volume of the homogenate was used for the serial dilutions. Quantification was performed by using the 10-fold serial dilution method;<sup>28</sup> 100  $\mu$ L of each dilution (either swab or tissue) was inoculated onto selective media (Chapman mannitol salt agar [Biokar Diagnostics] for *Staphylococcus aureus* or cefrimide agar [Merck Chemical] for *Pseudomonas aeruginosa*). The plates were incubated under aerobic conditions at 37 °C for 24 h, after which colony counts were performed. The isolates grown on Chapman mannitol salt agar were presumptively identified as *S. aureus* based on colony morphology and mannitol salt agar fermentation.<sup>9</sup> The isolates grown on cefrimide agar were presumptively identified as *P. aeruginosa* based on colony morphology.<sup>7</sup> Quantitative results are presented as the mean and standard deviation and expressed as logarithm-transformed values (log[cfu/swab] for swab samples and log[cfu/ulcer] for tissue samples). The data were compared by using a logarithmic scale owing to the wide variations in number of colony-forming units between cultures. Correlations were evaluated by the Pearson correlation coefficient, and the Fisher r-to-z method was used to calculate *P* values. A *P* value of less than 0.05 was considered significant. All data was entered into a spreadsheet program (Excel, Microsoft, Redmond, WA) for statistical analysis. Analytical statistics were performed by Analyse-it version 2.21 Excel 12+ (Analyse-it Software, Leeds, UK), a statistical add-in program for the spreadsheet program.

**Optimized final rodent wound-infection model. General protocol and wound-closure kinetics.** After every step of the procedure had been optimized, a final study (Figure 3) was designed by using 36 Wistar rats with chemically induced DM that were epilated by using cold-wax strips. Incisions were made, splinted, and dressed as previously described. Wounds were photographed from a 1.5-cm standard height by using a mounted digital microscope (SuperEyes 200 $\times$  USB Digital Microscope, Shenzhen Tak and Assistive Technology, Shenzhen, China; Figure 2 D), and the rats were divided randomly into 3 groups: inoculated with *S. aureus* (*n* = 12), inoculated with *P. aeruginosa* (*n* = 12), and negative control (*n* = 12). The ulcers of the animals in the infected groups were inoculated with either *S. aureus* or *P. aeruginosa* as previously described, whereas the ulcers of the negative control group were inoculated with sterile saline. On day 4 after wounding, the semiocclusive dressing was removed, the ulcer debrided and photographed, and a swab was obtained as previously described. The entire procedure, including debridement, was repeated on days 5, 8, and 11, and the splint chamber was filled twice daily with sterile saline from day 5 until the end of the study. Wound kinetics were quantified by using image-processing software (ImageJ, US National Institutes of Health, Bethesda, MD) to measure the wound area by planimetry; wound area was expressed as a percentage of the initial wound area. Results are expressed as the mean of the percentage in area of the original wound size. Comparisons between groups were performed by using 2-tailed Student *t* tests, and a *P* value of less than 0.01 was considered significant. All data were entered into the spreadsheet program, and analytical statistics were performed as described previously.

**Histologic analysis.** For each group, 6 rats each were euthanized by intraperitoneal injection of pentobarbital (200 mg) on

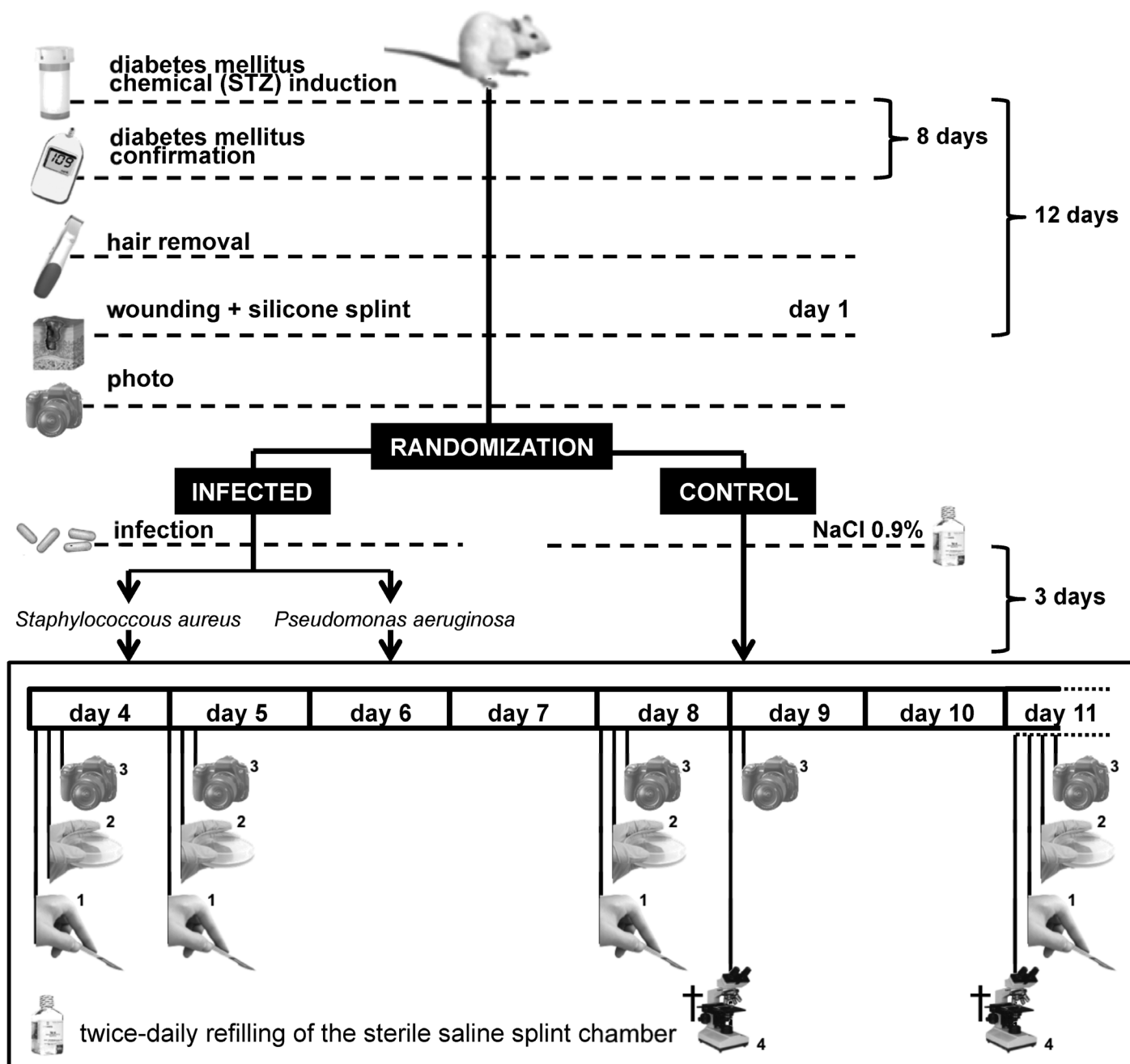


**Figure 3.** Final study design: optimized rodent wound infection model. Wistar rats each received a single intraperitoneal injection of streptozotocin; 8 d after injection, rats considered to be diabetic (fasting blood glucose greater than or equal to 250 mg/dL) were epilated by using cold-wax strips. At 4 d after epilation (study day 1), skin was disinfected, wounded, splinted, and photographed from a standard height. In addition, rats were divided randomly into 2 infected groups (inoculated with either *Staphylococcus aureus* or *Pseudomonas aeruginosa*) and 1 negative control group (inoculated with sterile saline). On study days 4, 5, 8, and 11, ulcers were (1) debrided, (2) swabbed, and (3) photographed. From day 5 until the end of the study, splint chambers were filled twice daily with sterile saline. On study days 9 and 11, half of the animals in each group were (4) euthanized, and each ulcer was processed for histologic analysis.

days 9 and 11, and each ulcer (including a 0.5-cm skin border) was harvested in its entirety by using sterile surgical scissors and placed in a tube. The sample was fixed overnight in 10% buffered formalin solution, after which the tissue was trimmed and cut through at the widest margin, embedded in paraffin, and sectioned in 3- $\mu$ m increments. Sections were made perpendicular to

the anteroposterior axis and perpendicular to the surface of the wound. For each wound, 2 serial sections were placed on a slide and stained with hematoxylin and eosin. Under light microscopy, the sections were photographed by using an upright bright-field microscope equipped with a color camera (model DM2500, Leica Microsystems, Wetzlar, Germany) at 50 $\times$  magnification.

Panoramic cross-sectional digital images of each wound were prepared by using professional image-editing software (Photoshop CS2, Adobe Systems, San Jose, CA). The images were analyzed for epithelial gap (EG), dermal gap (DG), and total granulation tissue (GT) area by using image-processing software. EG was defined as the distance between the advancing edges of clear, multiple-layer neoepidermis,<sup>16,36</sup> and its size was measured in millimeters, with an EG of 0 representing a completely reepithelialized wound. DG was defined as the distance between uninjured dermis on both sides of the wound<sup>16,36</sup> and was measured in millimeters. GT area was calculated by computerized morphometric analysis<sup>16</sup> and expressed in square millimeters. The results are presented as mean  $\pm$  SEM. Comparisons between groups were performed by using 2-tailed Student *t* tests, and a *P* value of less than 0.05 was considered significant. All data were entered into the spreadsheet program and analytical statistics were performed as described previously.

## Results

**Animals and induction of DM.** We induced diabetes in 98 male Wistar rats with a success rate of 81.6%. Of the 80 successfully induced rats, 3.8% died prior to the end of the study; at necropsy, no significant gross pathology was noted. There was no mortality during the optimized final study. For the final study, 77 animals (78.6% of the number of rats induced initially) were used. At the time of euthanasia, all rats were confirmed to have fasting glucose levels of at least 250 mg/dL, and the mean weight loss was 18.10%  $\pm$  2.35%.

**Optimization study 1: hair removal.** Depilation by using a straight razor gave the worst hair density and skin damage results throughout the 15 d of the experiment (Figure 4). Although cold wax tended to cause increased immediate (day 1) epithelial injury, as measured by the skin-damage index, compared with that from the depilatory cream, this pattern was completely reversed by day 4. Epilatory hair removal by using cold wax achieved more prolonged results than did the depilatory methods (straight razor or depilatory cream), as evaluated by using the hair-density index, with less skin damage after day 4, which was the optimal day for infection.

**Optimization study 2: prevention of unintentional critical colonization.** This experiment examined methods for preventing unintentional critical bacterial colonization. The use of a combined approach (washing with sterile saline, followed by disinfection with povidone-iodine and washing with isopropyl alcohol after 10 min contact time) produced the best results (Table 1), with only 1 of the 6 control wounds having a swab colony count that exceeded 3 logs ( $4.6 \times 10^5$  cfu/swab). No dressing or splint was lost during the experiment.

**Optimization study 3: assessment of wound bioburden.** The average colony count in swab samples (Table 2) was similar between the 2 species:  $5.67 \pm 0.16$  log(cfu/swab) for *S. aureus* and  $5.65 \pm 0.26$  log(cfu/swab) for *P. aeruginosa*. The colony counts in tissue samples differed between the 2 species by 0.16 log(cfu/ulcer) but this difference was not statistically significant (2-tailed *t* test, data not shown). The one-point quantitative swab method underestimated the number of bacteria in the wound bed by  $1.79 \pm 0.10$  log(cfu) for *S. aureus* and  $1.97 \pm 0.16$  log(cfu) for *P. aeruginosa*. The Pearson correlation coefficient (*r*) between swab and tissue colony counts was 0.810 (95% confidence interval, 0.143 to 0.971; *P* = 0.025) for *S. aureus* and 0.780 (95% confidence inter-

**Table 1.** Evaluation of 3 strategies for preventing unintentional critical colonization<sup>a</sup>

Bacteria count	Sterile saline (n = 6)	Sterile saline followed by 10 min of 10% povidone-iodine (n = 6)	Sterile saline, 10 min of 10% povidone-iodine, and 70% isopropanol (n = 6)
$\leq 10^3$	2 (33.3%)	3 (50.0%)	5 (83.3%)
$> 10^3$	4 (66.7%)	3 (50.0%)	1 (16.7%)

<sup>a</sup>Bacterial count  $> 10^3$  cfu/swab on any given study day

val, 0.065 to 0.966; *P* = 0.037) for *P. aeruginosa*, suggesting a strong relationship between the 2 independent measures. This statistical correlation was not observed when data from the 2 infected groups were combined.

**Optimized rodent wound-infection model. Wound-closure kinetics.** In the final wound-infection model study, the control group showed continuous reduction of the wound area that was enhanced after mechanical debridement (Figure 5). During the first 4 d after infection, the wound area increased on average to 110.6% of the original size in the *P. aeruginosa* group and 102.3% of the original size in the *S. aureus* group. After the first debridement, the wound area began to decrease, paralleling a decrease in the microbial load. There was a statistically significant difference (*P* < 0.01) in wound area between the negative control and both infected groups on days 8 and 9; on day 11, only the difference between the negative control and *Pseudomonas aeruginosa* groups remained significant. Microbial load was similar between the 2 infected groups (5.66 compared with 5.54 log[CFU/swab]) on day 4 and did not differ significantly on days 5, 8, and 11.

**Histologic analysis.** Both EG and DG decreased (*P* < 0.01) as the GT area increased in all groups from day 9 to day 11 (Figure 6). On day 9, EG closure was significantly delayed in infected groups compared with controls (*S. aureus*,  $0.12 \pm 0.06$  mm; *P. aeruginosa*,  $1.3 \pm 0.15$  mm; control,  $1.55 \pm 0.15$  mm; *P* < 0.01). By day 11, all wounds were completely reepithelialized, except for a single ulcer in the rats inoculated with *P. aeruginosa*. GT area did not differ between groups on either day 9 or 11. However, DG closure followed wound contraction, as evaluated by digital planimetry. Wounds of infected rats showed significantly less DG closure than did those of control rats on days 9 (*S. aureus*,  $1.88 \pm 0.09$  mm; *P. aeruginosa*,  $2.93 \pm 0.08$  mm; control,  $3.17 \pm 0.15$  mm; *P* < 0.01) and 11 (*S. aureus*,  $1.30 \pm 0.16$  mm; *P. aeruginosa*,  $2.20 \pm 0.15$  mm; control,  $2.43 \pm 0.06$  mm; *P* < 0.01). DG closure did not differ significantly between infected groups.

## Discussion

The impairment of wound healing by DM, which is potentiated by infection, causes a significant amount of human morbidity and mortality worldwide<sup>14,30</sup> and has prompted the investigation of new TAT approaches. Although swine are thought to be the ideal large animal model for cutaneous disease,<sup>18</sup> the use of rodents overcomes several of its disadvantages (for example, size, cost, housing, husbandry, and reagent validation). Therefore, rodents are still the model of choice for research purposes in this area. However, there are no standardized wound-infection models for testing TAT.

One well-known rodent model<sup>16</sup> is a splinted, excisional wound-healing model that involves genetically diabetic mice (db/db mice). In contrast, we used male Wistar rats in which DM

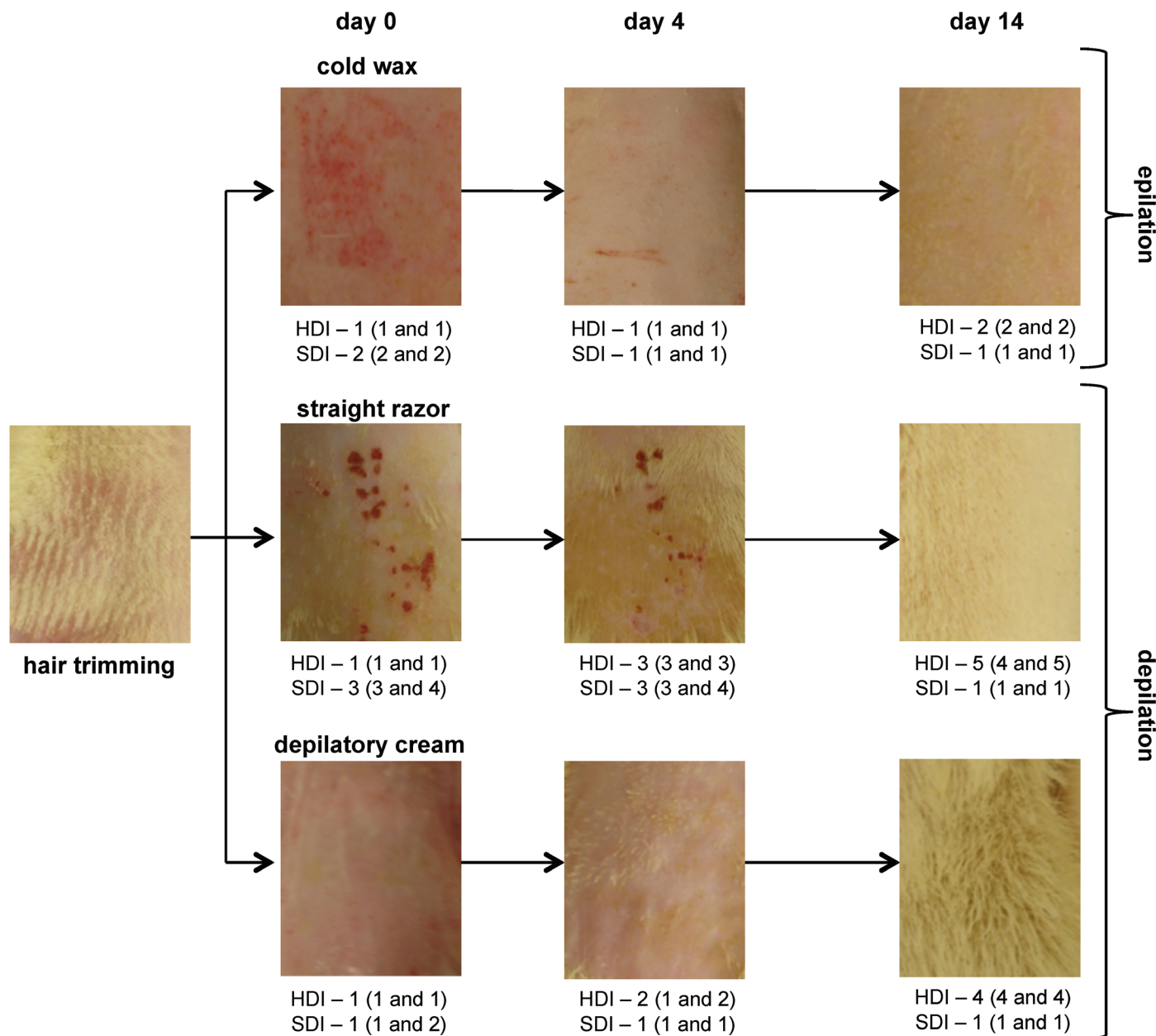


**Figure 4.** Results of the hair-removal optimization study. After dorsal hair trimming, rats were divided into 3 groups: straight razor, depilatory cream, and cold wax. Photographs were taken immediately, 4 d, and 14 d after removal procedures; 3 independent observers evaluated 2 parameters: hair-density index (HDI) and skin-damage index (SDI). Results are expressed as median (first and third quartiles).

had been chemically induced as a rodent model. Rats are a widely used biomedical research animal and currently the primary model for many preclinical tests, including those in the DM field.<sup>22</sup> Although the use of rat models has declined in the last decade, mainly due to broad advances in the development of mouse genetic technologies, rats still afford many advantages over mice, primarily in regard to size and behavioral characteristics.<sup>20</sup> In our case, the adhesive-tape jacket needed to prevent dressing loss and subsequent unintentional critical colonization would be impossible to adapt to a smaller rodent. Moreover, we expected our studies to involve frequent, nonpainful procedures. Rats often are easier to train and handle than are mice,<sup>34</sup> obviating the need

for inhalant anesthesia before procedures and reducing the associated time, distress, and mortality risks. Except for during the initial epilation and wounding procedures, the rats in our current study were restrained simply by placing a surgical drape over the rat's head to maintain immobilization in the absence of any identifiable behavioral stress signs.

We have used streptozotocin-induced diabetic Wistar rats rather than one of the available rat genetic models. Although genetic models offer some undisputed advantages, they are of limited availability and are expensive for regular screening studies of wound healing related to DM.<sup>41</sup> Further, the most common and readily available of genetically diabetic rats are obese to the point

**Table 2.** Bacterial colony counts (log[CFU]) from tissue or swab culture of wounds infected with *Staphylococcus aureus* or *Pseudomonas aeruginosa*

	log(cfu) (mean ± 1 SD)			Pearson R	P <sup>a</sup> (95% confidence interval)
	Tissue	Swab	Tissue – swab		
<i>S. aureus</i> (n = 7)	7.46 ± 0.17	5.67 ± 0.16	1.79 ± 0.10	0.810	0.025 (0.143–0.971)
<i>P. aeruginosa</i> (n = 7)	7.62 ± 0.18	5.65 ± 0.26	1.97 ± 0.16	0.780	0.037 (0.065–0.966)
Overall (n = 14)	7.54 ± 0.19	5.66 ± 0.21	1.88 ± 0.16	0.743	nonsignificant

<sup>a</sup>P value as calculated by the Fisher r-to-z method

that excisional wound closure is impeded not only by physiologic dysfunction but also by excess subcutaneous fat.<sup>11</sup>

Streptozotocin targets and inhibits pancreatic β-cell function without affecting the exocrine function and produces a DM type 1 phenotype with residual insulin secretion that enables animals to live longer than do genetic models before insulin treatment is needed. However, in addition to this biochemical deficit, this chemical agent causes other effects, such as altered T cell function and decreased macrophage phagocytosis, which also may contribute to impaired healing.<sup>17,36,38</sup> Nevertheless, the streptozotocin model is one of the most suitable for use in wound healing studies, allowing accurate quantification of the main aspects of a healing wound such as wound closure, reepithelialization, and GT formation. In addition, we used male rats, whose pancreatic islet β cells are more prone to streptozotocin-induced cytotoxicity than are those of female rats<sup>52</sup> and which have 40% stronger skin than do female rats, due to a much thicker dermis.<sup>51</sup> Our DM-induction rate exceeded 80%, as expected for the protocol,<sup>52</sup> and the postinduction mortality rate was low (less than 5%).

The silicone splint was used in previous models because it minimized wound contraction without affecting the rate of reepithelialization, thus better recapitulating the repair mechanisms underlying human wound healing.<sup>51</sup> In our current study, the splint had the additional benefit of creating a sealed artificial chamber over the wound, maintaining sterility at the wound site and allowing the establishment of a monoculture infection while enabling the application of products in a liquid vehicle. We filled this chamber twice daily with sterile saline, which provided a wet wound microenvironment beneficial to wound healing.<sup>49</sup> Sterile saline is also the most frequently used negative TAT control. The influence of the splint and dressing maintenance on wound closure has been reported as a problem.<sup>16,36</sup> When the dressing is breached, the wound becomes contaminated, and splint loss is easier. Once animals lose the splint, wound closure occurs more rapidly. All of these factors can lead to the exclusion of animals from the study; therefore, meticulous application and maintenance of the dressing that protects the splint is an essential aspect of model standardization. To prevent dressing loss, we introduced a jacket made from adhesive tape. With twice-daily evaluation for the integrity of the adhesive-tape jacket and the addition of reinforcement whenever deemed necessary, we had a 100% success rate of maintaining the dressing and splint to the end of the experiment. The jacket seemed to be well tolerated by the rats, which exhibited no overt signs of distress.

Rodent skin is covered with dense hair that undergoes a defined cycle of hair growth similar to that of human hair.<sup>11</sup> Although hair removal protocols are described in detail only infrequently in studies, hair regrowth has been reported as an impediment to splint and dressing skin adherence, resulting in the

failure of skin contraction restriction and consequent exclusion of animals from the study.<sup>53</sup> This problem is particularly important in wound infection models, because razor shaving produces microscopic cuts in the epidermis, and hair growth around the wound site acts as a wick, both of which increase the risk of wound contamination. Cold waxing, as indicated by the hair-density index we used here, was more effective than were shaving or chemical depilatories because waxing removed the hair from beneath the skin surface.<sup>2</sup> This improvement in limiting hair growth was made at the expense of persistent skin lesions. However, although cold wax tended to cause more immediate (day 1) epithelial injury, as measured by the skin-damage index, than did depilatory cream, this effect was completely reversed by day 4. This outcome is consistent with previous skin electrical potential studies,<sup>2</sup> which showed that waxing causes stratum corneum damage with an immediate loss of cutaneous barrier function and has a rapid and apparently complete recovery by the fifth day after treatment. From our optimization study and based on the previously cited skin electrical potential study,<sup>2</sup> we decided to use cold waxing epilation in our final study at 4 d before wounding. This strategy prevented regrowth of hair throughout the course of the experiment and maintained the barrier function of the healthy surrounding skin.

The conversion of an excisional wound model to a wound-infection model is simple enough. The addition of a known concentration of virulent bacteria to the wound bed establishes infection in the test group,<sup>18</sup> but the most difficult problem to solve is the prevention of unintentional critical colonization or infection. Although sterilization of the wound is impossible, the use of strict measures can prevent colonization by pathogenic or normal skin flora microorganisms beyond a certain threshold, above which there may be impairment to wound healing. We and others<sup>5,33</sup> consider this limit to be a tissue microbial load of 10<sup>5</sup> cfu/g tissue or 10<sup>3</sup> cfu/swab. A bioburden below this threshold does not seem to impair tissue repair and frequently has a positive effect on wound healing.<sup>23</sup> One potential criticism of our current study is that we did not include a chlorhexidine-based antiseptic solution test group; this type of antiseptic is considered to be ideal for wound infection prevention because of its persistent activity that prevents regrowth of microorganisms for at least 24 h.<sup>27</sup> This characteristic was the reason we did not include this type of disinfectant in our model: we would have had to pretreat the infection test group with the antiseptic solution, and its residual antiseptic activity might have limited the development of infection. We chose to use 10% povidone-iodine and 70% isopropyl alcohol, because these agents have an immediate bactericidal action but minimal residual activity.<sup>26</sup> This strategy has been adopted in another animal model of diabetic wound infection.<sup>19</sup>



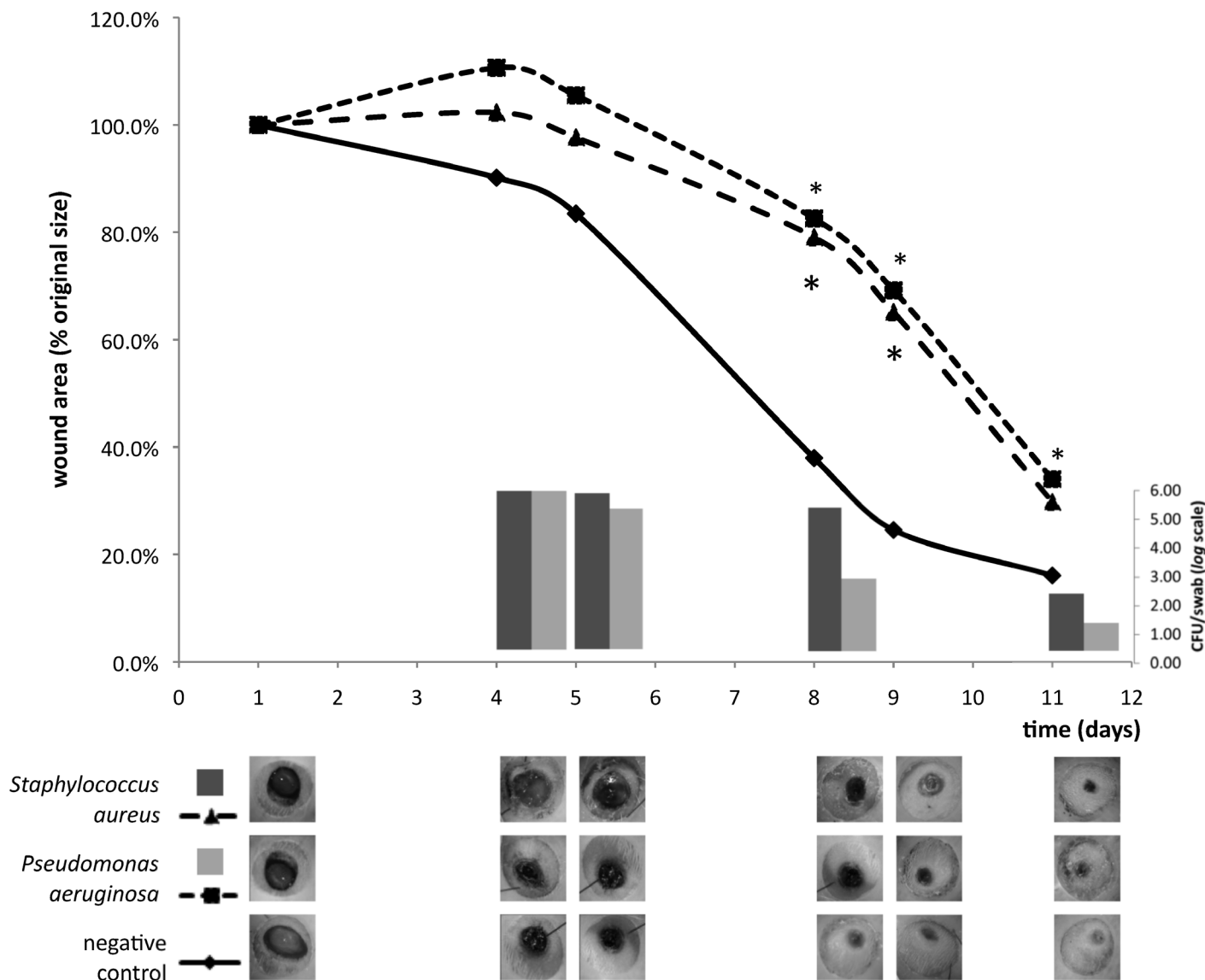


**Figure 5.** Results of the final wound-infection model study. The line graph illustrates wound healing kinetics of the infected (*Staphylococcus aureus* or *Pseudomonas aeruginosa*) and negative control groups. Each point represents the mean of the percentage in area of the original wound size. After day 4, wound area decreased progressively and was enhanced after mechanical debridement. Wound area differed significantly (\*,  $P < 0.01$ ) between the negative control and both infected groups on days 8 and 9 and between the negative control and *Pseudomonas aeruginosa*-inoculated groups on day 11. The bar graph illustrates microbial load (from quantitative swab-sample cultures and expressed in no. of cfu per swab [log scale]) between the 2 infected groups on days 4, 5, 8, and 11. The *Staphylococcus aureus*-inoculated group showed a trend ( $0.05 < P < 0.10$ ) toward increased microbial load on days 5, 8, and 11. The lower panel contains macrophotographs of wounds from a representative rat in each group at each time point.

One of the greatest controversies in wound management is the usefulness of quantitative swab cultures for predicting the presence of wound infection. This method has received criticism because it is thought to estimate wound-surface microbial numbers only and not deep-tissue numbers.<sup>5</sup> However, several studies in humans and animals have demonstrated high sensitivity (93.5% to 100%) and good specificity (76.3% to 94.2%) and accuracy (approximately 90% to 99%) when compared with tissue-biopsy quantitative cultures.<sup>44,45</sup> In an experimental acute-wound rat model, a tissue count of  $10^5$  cfu/g was equivalent to a count of

$10^3$  cfu/mL obtained from a moist swab;<sup>4</sup> another study<sup>45</sup> demonstrated that compared with biopsy cultures, one-point quantitative swab cultures detected similar types of microorganisms but underestimated bacterial numbers by a factor of 2 logs. These studies suggest that the quantitative swab method of collection and culturing is acceptable, given its correlation with the invasive method. The invasive method was strongly contraindicated in the model we developed because our study required serial evaluations of the bioburden, along with planimetry by digital photography and a final histologic evaluation. Because these measures

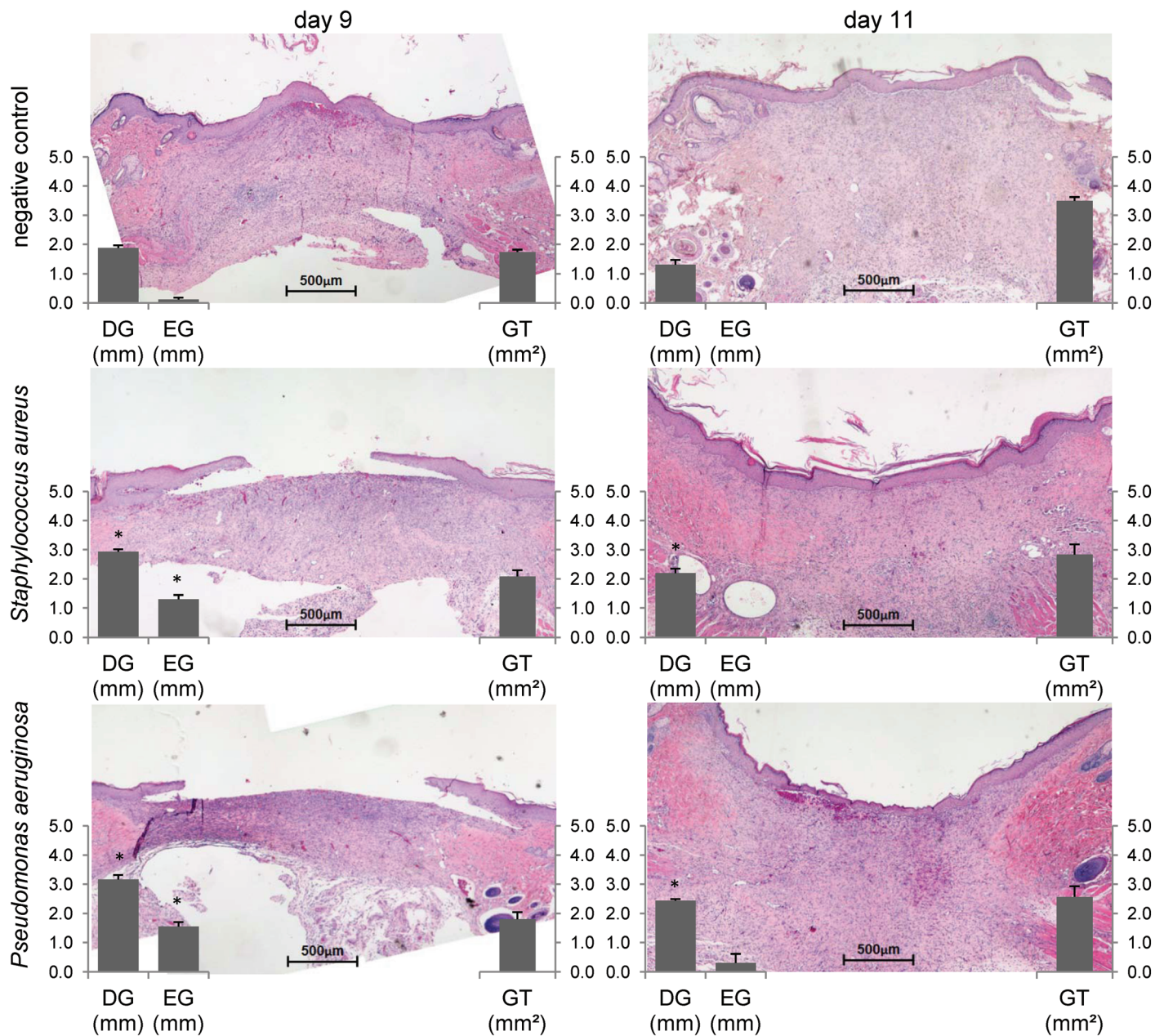


**Figure 6.** Quantitative histologic evaluation of epithelial gap (EG), dermal gap (DG), and granulation tissue (GT) area in the negative control and both infected (*Staphylococcus aureus* or *Pseudomonas aeruginosa*) groups on days 9 and 11. On day 9, EG closure in both infected groups was significantly (\*,  $P < 0.01$ ) delayed compared with that in the control group. On days 9 and 11, wounds in the infected groups showed significantly (\*,  $P < 0.01$ ) less DG closure than did the control group. Original magnification,  $\times 50$ .

constituted the final endpoints and would have been influenced by the wound-bed trauma induced by serial biopsies, we opted for swabbing.

Many methods<sup>3</sup> have been described for swab collection (10-point diagonal method, 1-cm<sup>2</sup>-area sampling method, and one-point rotation method), but none has gained universal acceptance. In the current study and in accordance with others,<sup>45</sup> we selected the one-point method because of the relatively small size of the wounds and to better avoid contamination with

periwound flora. In a murine DM wound-healing model using quantitative cultures and transmission electron microscopy studies,<sup>54</sup> the majority of bacteria were in the scab above the wound bed rather than in the wound tissue. In addition, ulcer debridement (that is, the removal of the scab), which is essential to the model we developed, reproduced the current clinical practice of wound debridement previous to microbiologic sampling<sup>5</sup> and theoretically provided an improved estimate of deep-tissue bacterial numbers. Although the numbers of colonies obtained from

swab and tissue samples varied, both samples were correlated logarithmically for each bacterium. Our data indicated that the one-point swab culture yielded an average 1.9 log(cfu) underestimation of colony counts compared with those of the tissue cultures, consistent with the results of several other clinical and experimental studies.<sup>4,29,45</sup> Surprisingly, we found that when *P. aeruginosa* and *S. aureus* groups were pooled before evaluation, this correlation could not be reestablished. Our results, which show underestimation of *P. aeruginosa* swab samples relative to *S. aureus* swab samples, may be explained by differential distribution of the 2 bacteria in the wound. This notion is in line with a previous study,<sup>15</sup> in which confocal laser scanning microscopy of clinical wound-biopsy specimens demonstrated that the distance from *P. aeruginosa* aggregates to the wound surface was greater than that of *S. aureus* aggregates, leading to underestimation of *P. aeruginosa* in swab samples. This result supports the possibility that factors intrinsic to each pathogenic bacteria contribute, as does sampling technique, to the differences reported in studies comparing swab and tissue-sample quantitative cultures. Finally, the choice of selective media (cetrimide or Chapman mannitol salt agar) is important, because using the proper medium is essential for the correct evaluation of target pathogens<sup>5</sup> and to prevent concurrent colonization by other microorganisms. The noninvasiveness of the quantitative swab, which allowed concomitant debridement and revealed a strong correlation with tissue sampling, made this method ideal for use in our rodent wound-infection model.

After optimizing each step of the process, we designed a protocol allowing the simultaneous and serial assessment of microbial load (by using quantitative swab-sample cultures) and the kinetics of wound closure (through digital photography and computerized planimetry software) and a well-defined and easily repeatable quantitative histologic evaluation. It was our requirement that the model not only accurately paralleled the healing of infected wounds in humans but also the current treatment standard of care. Sharp debridement is standard procedure in wound management, and there is no clinical or experimental rationale for using TAT products in its absence.<sup>25</sup> Debridement converts the molecular and cellular environment of a chronic wound to that of an acute, healing wound through the removal of scabs and debris. Many studies<sup>37,50,54</sup> indicate that debridement plays an important role in removing bioburden and enhancing cicatrization, and its frequency is directly related to the rate of healing.<sup>43</sup> Furthermore and most importantly, debridement has been shown in several models to open a time-dependent window for TAT use.<sup>50</sup> Debridement led to a significant decrease in the resistance of the bioburden to TAT for as long as 24 h, with resistance increasing to reach the original resistance levels at 72 h.

Our current study using a rat model replicates the current debridement protocol for infected diabetic ulcers.<sup>42</sup> Initial debridement (day 4) removed a cellular burden of dead and senescent cells and excessive bacterial load; additional maintenance debridement (days 5 and 8) maintained the wound environment and the readiness of the wound bed for healing. The effects of debridement are manifest in our model: first, by limiting the increase in the size of the wound area after day 4, and second, by accelerating wound-healing kinetics as revealed by the inflections in the infected-wound healing curve, which becomes parallel to the control curve from the third debridement onwards. In the current study, macroscopic wound closure showed a similar trend when compared with that of the EG and DG measured in histologic

specimens among the control and infected groups. There was not, however, a statistically significant difference in GT area among groups. This result is probably related to an increase in collagenolytic activity in the wound, generating increased feedback synthesis.<sup>8</sup> Qualitative differences in GT between groups may exist, and additional studies, such as complementary breaking-strength measurements, would be of interest. From the analysis of the planimetry and histologic data, we can conclude that in our model, the best time to evaluate differences between the infected and control groups is day 9, and TAT studies probably will not benefit from a longer period of evaluation. In addition, DG closure is a better parameter than is GT area for evaluating the histologic level of contraction of the wound.

In summary, we optimized a new wound infection model in chemically induced diabetic Wistar rats. This model can be used to investigate new approaches to TAT. The model has numerous benefits: the necessary materials and techniques are simple, reproducible, and practical for experiments with large sample sizes. Furthermore, in light of the analogies to human-infected wound healing and treatment, this model can serve as a valid alternative for applied research.

## Acknowledgments

We thank the Instituto de Medicina Molecular Animal Facility staff, and José Rino, António Temudo and Raquel Barbosa for providing technical support. This work was supported by TechnoPhage.

## References

1. **Ahn ST, Mustoe TA.** 1990. Effects of ischemia on ulcer wound healing: a new model in the rabbit ear. *Ann Plast Surg* **24**:17–23.
2. **Ando HY, Escobar A, Schnaare RL, Sugita ET.** 1983. Skin potential changes in the guinea pig due to depilation and the repeated application of polyethylene glycol and retinoic acid. *J Soc Cosmet Chem* **34**:159–169.
3. **Bonham PA.** 2009. Swab cultures for diagnosing wound infections: a literature review and clinical guideline. *J Wound Ostomy Continence Nurs* **36**:389–395.
4. **Bornside GH, Bornside BB.** 1979. Comparison between moist swab and tissue biopsy methods for quantitation of bacteria in experimental incisional wounds. *J Trauma* **19**:103–105.
5. **Bowler PG, Duerden BI, Armstrong DG.** 2001. Wound microbiology and associated approaches to wound management. *Clin Microbiol Rev* **14**:244–269.
6. **Braiman-Wiksmann L, Solomonik I, Spira R, Tennenbaum T.** 2007. Novel insights into wound healing sequence of events. *Toxicol Pathol* **35**:767–779.
7. **Brown VI, Lowbury EJ.** 1965. Use of improved cetrimide agar medium and other culture methods for *Pseudomonas aeruginosa*. *J Clin Pathol* **18**:752–756.
8. **Bucknall TE.** 1980. The effect of local infection upon wound healing: an experimental study. *Br J Surg* **67**:851–855.
9. **Chapman GH.** 1946. A single culture medium for selective isolation of plasma-coagulating staphylococci and for improved testing of chromogenesis, plasma coagulation, mannitol fermentation, and the Stone reaction. *J Bacteriol* **51**:409–410.
10. **Council of the European Communities.** Council Directive 86/609/EEC of 24 November 1986 on the approximation of laws, regulations and administrative provisions of the Member States regarding the protection of animals used for experimental and other scientific purposes. *Off J Eur Communities* **L358**:1–28.
11. **Davidson JM.** 1998. Animal models for wound repair. *Arch Dermatol Res* **290** Suppl:S1–S11.
12. **El-Aziz A, El-Banna T, Abo-Kamar A, Ghazal A, AboZahra R.** 2010. In vitro and in vivo activity of some antibiotics against staphylococcal

- biofilm and planktonic cells isolated from diabetic foot infections. *Journal of American Science* 6:760–770.
13. Falagas ME, Koletsis PK, Bliziotis IA. 2006. The diversity of definitions of multidrug-resistant (MDR) and pandrug-resistant (PDR) *Acinetobacter baumannii* and *Pseudomonas aeruginosa*. *J Med Microbiol* 55:1619–1629.
  14. Falanga V. 2005. Wound healing and its impairment in the diabetic foot. *Lancet* 366:1736–1743.
  15. Fazli M, Bjarnsholt T, Kirketerp-Moller K, Jorgensen B, Andersen AS, Krogfelt KA, Givskov M, Tolker-Nielsen T. 2009. Nonrandom distribution of *Pseudomonas aeruginosa* and *Staphylococcus aureus* in chronic wounds. *J Clin Microbiol* 47:4084–4089.
  16. Galiano RD, Michaels J 5th, Dobryansky M, Levine JP, Gurtner GC. 2004. Quantitative and reproducible murine model of excisional wound healing. *Wound Repair Regen* 12:485–492.
  17. Goodson WH 3rd, Hung TK. 1977. Studies of wound healing in experimental diabetes mellitus. *J Surg Res* 22:221–227.
  18. Greenhalgh DG. 2005. Models of wound healing. *J Burn Care Rehabil* 26:293–305.
  19. Hirsch T, Spielmann M, Zuhaili B, Koehler T, Fossum M, Steinau HU, Yao F, Steinstraesser L, Onderdonk AB, Eriksson E. 2008. Enhanced susceptibility to infections in a diabetic wound healing model. *BMC Surg* 8:5.
  20. Huang G, Tong C, Kumbhani DS, Ashton C, Yan H, Ying QL. 2011. Beyond knockout rats: new insights into finer genome manipulation in rats. *Cell Cycle* 10:1059–1066.
  21. Institute for Laboratory Animal Research. 2011. Guide for the care and use of laboratory animals, 8th ed. Washington (DC): National Academies Press.
  22. Lee JH, Yang SH, Oh JM, Lee MG. 2010. Pharmacokinetics of drugs in rats with diabetes mellitus induced by alloxan or streptozocin: comparison with those in patients with type I diabetes mellitus. *J Pharm Pharmacol* 62:1–23.
  23. Levenson SM, Kan-Gruber D, Gruber C, Molnar J, Seifter E. 1983. Wound healing accelerated by *Staphylococcus aureus*. *Arch Surg* 118:310–320.
  24. Lipsky BA, Berendt AR, Deery HG, Embil JM, Joseph WS, Karchmer AW, LeFrock JL, Lew DP, Mader JT, Norden C, Tan JS. 2004. Diagnosis and treatment of diabetic foot infections. *Clin Infect Dis* 39:885–910.
  25. Lipsky BA, Hoey C. 2009. Topical antimicrobial therapy for treating chronic wounds. *Clin Infect Dis* 49:1541–1549.
  26. Maki DG, Ringer M, Alvarado CJ. 1991. Prospective randomised trial of povidone-iodine, alcohol, and chlorhexidine for prevention of infection associated with central venous and arterial catheters. *Lancet* 338:339–343.
  27. Mayhall CG. 2004. Hospital epidemiology and infection control. Philadelphia (PA): Lippincott Williams and Wilkins.
  28. Murray PR, Baron EJ, Jorgensen JH, Pfaller MA, Tenover FC, Tenover FC. 2003. Manual of clinical microbiology. Washington (DC): ASM Press.
  29. Neil JA, Munro CL. 1997. A comparison of 2 culturing methods for chronic wounds. *Ostomy Wound Manage* 43:20–22, 24, 26 passim.
  30. Pecoraro RE, Reiber GE, Burgess EM. 1990. Pathways to diabetic limb amputation. Basis for prevention. *Diabetes Care* 13:513–521.
  31. Portuguese Agricultural Ministry. *Portaria no. 1005/92 of 23 October* on the protection of animals used for experimental and other scientific purposes. *Diário da República I – Série B*, 245:4930–4942.
  32. Prompers L, Huijberts M, Apelqvist J, Jude E, Piaggese A, Bakker K, Edmonds M, Holstein P, Jirkovska A, Mauricio D, Tennvall GR, Reike H, Spraul M, Uccioli L, Urbancic V, Van Acker K, Van Baal J, Van Merode F, Schaper N. 2007. Optimal organization of health care in diabetic foot disease: introduction to the Eurodiale study. *Int J Low Extrem Wounds* 6:11–17.
  33. Robson MC, Lea CE, Dalton JB, Hegggers JP. 1968. Quantitative bacteriology and delayed wound closure. *Surg Forum* 19:501–502.
  34. Rodier PM. 1976. Critical periods for behavioral anomalies in mice. *Environ Health Perspect* 18:79–83.
  35. Romana-Souza B, Nascimento AP, Monte-Alto-Costa A. 2009. Propranolol improves cutaneous wound healing in streptozotocin-induced diabetic rats. *Eur J Pharmacol* 611:77–84.
  36. Scherer SS, Pietramaggiore G, Mathews JC, Chan R, Fiorina P, Orgrill DP. 2008. Wound healing kinetics of the genetically diabetic mouse. *Wounds* 20:18–28.
  37. Schultz GS, Sibbald RG, Falanga V, Ayello EA, Dowsett C, Harding K, Romanelli M, Stacey MC, Teot L, Vanscheidt W. 2003. Wound bed preparation: a systematic approach to wound management. *Wound Repair Regen* 11 Suppl 1:S1–S28.
  38. Seifter E, Rettura G, Padawer J, Stratford F, Kambosos D, Levenson SM. 1981. Impaired wound healing in streptozotocin diabetes. Prevention by supplemental vitamin A. *Ann Surg* 194:42–50.
  39. Shi CM, Nakao H, Yamazaki M, Tsuboi R, Ogawa H. 2007. Mixture of sugar and povidone-iodine stimulates healing of MRSA-infected skin ulcers on db/db mice. *Arch Dermatol Res* 299:449–456.
  40. Singh N, Armstrong DG, Lipsky BA. 2005. Preventing foot ulcers in patients with diabetes. *JAMA* 293:217–228.
  41. Srinivasan K, Ramarao P. 2007. Animal models in type 2 diabetes research: an overview. *Indian J Med Res* 125:451–472.
  42. Steed DL, Attinger C, Colaizzi T, Crossland M, Franz M, Harkless L, Johnson A, Moosa H, Robson M, Serena T, Sheehan P, Veves A, Wiersma-Bryant L. 2006. Guidelines for the treatment of diabetic ulcers. *Wound Repair Regen* 14:680–692.
  43. Steed DL, Donohoe D, Webster MW, Lindsley L. 1996. Effect of extensive debridement and treatment on the healing of diabetic foot ulcers. Diabetic Ulcer Study Group. *J Am Coll Surg* 183:61–64.
  44. Stotts NA. 1995. Determination of bacterial burden in wounds. *Adv Wound Care* 8:46–52.
  45. Sullivan PK, Conner-Kerr TA, Hamilton H, Parrish-Smith E, Tefertiller C, Webb A. 2004. Assessment of wound bioburden development in a rat acute wound model—quantitative swab versus tissue biopsy. *Wounds* 16:115–123.
  46. Toker S, Gulcan E, Cayc MK, Olgun EG, Erbilien E, Ozay Y. 2009. Topical atorvastatin in the treatment of diabetic wounds. *Am J Med Sci* 338:201–204.
  47. Tsuboi R, Rifkin DB. 1990. Recombinant basic fibroblast growth factor stimulates wound healing in healing-impaired db/db mice. *J Exp Med* 172:245–251.
  48. Velerand P, Theopold C, Hirsch T, Bleiziffer O, Zuhaili B, Fossum M, Hoeller D, Gheerardyn R, Chen M, Visovatti S, Svensson H, Yao F, Eriksson E. 2008. Impaired wound healing in an acute diabetic pig model and the effects of local hyperglycemia. *Wound Repair Regen* 16:288–293.
  49. Vogt PM, Andree C, Breuing K, Liu PY, Slama J, Helo G, Eriksson E. 1995. Dry, moist, and wet skin wound repair. *Ann Plast Surg* 34:493–499, discussion 499–500.
  50. Wolcott RD, Rumbaugh KP, James G, Schultz G, Phillips P, Yang Q, Watters C, Stewart PS, Dowd SE. 2010. Biofilm maturity studies indicate sharp debridement opens a time-dependent therapeutic window. *J Wound Care* 19:320–328.
  51. Wong VW, Sorkin M, Glotzbach JP, Longaker MT, Gurtner GC. 2011. Surgical approaches to create murine models of human wound healing. *J Biomed Biotechnol* 2011:969618.
  52. Wu K, Huan Y. 2008. Streptozotocin-induced diabetic models in mice and rats. *Curr Protoc Pharmacol* 40:5.47.1–5.47.14.
  53. Wu Y, Chen L, Scott PG, Tredget EE. 2007. Mesenchymal stem cells enhance wound healing through differentiation and angiogenesis. *Stem Cells* 25:2648–2659.
  54. Zhao G, Hochwalt PC, Usui ML, Underwood RA, Singh PK, James GA, Stewart PS, Fleckman P, Olerud JE. 2010. Delayed wound healing in diabetic (db/db) mice with *Pseudomonas aeruginosa* biofilm challenge: a model for the study of chronic wounds. *Wound Repair Regen* 18:467–477.